AAS 09-074

MAGNETIC RATE DAMPING FOR SATELLITES IN LEO

Peter Zentgraf[1], Domenico Reggio[2]

[1]ESA, [2]Astrium GmbH

32nd ANNUAL AAS GUIDANCE AND CONTROL CONFERENCE

January 31 - February 4, 2009
Breckenridge, Colorado

Sponsored by
Rocky Mountain Section

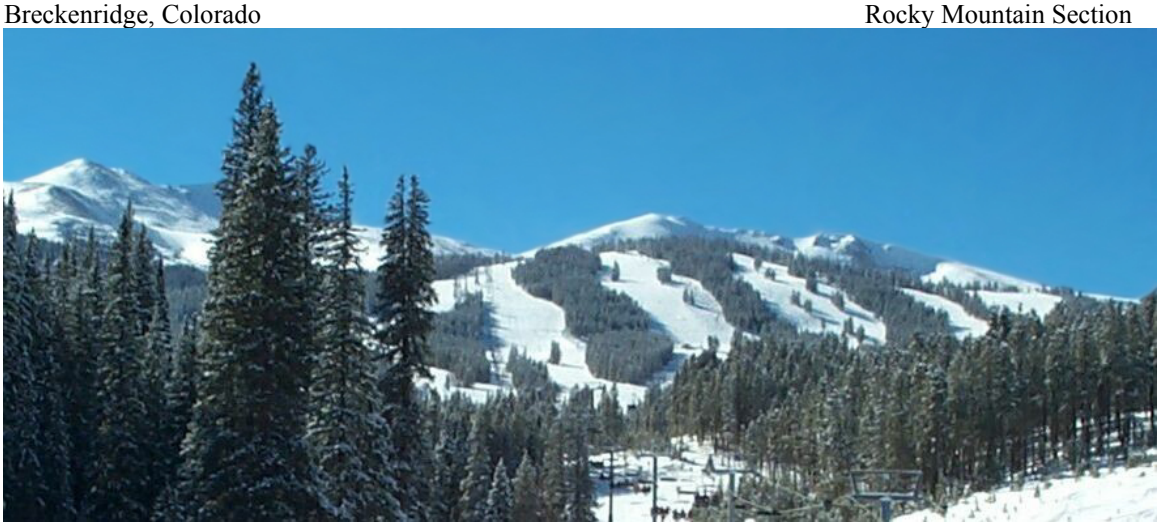

AAS Publications Office, P.O. Box 28130 - San Diego, California 92198

AAS 09-074

MAGNETIC RATE DAMPING FOR SATELLITES IN LEO

Peter Zentgraf[1], Domenico Reggio [2]

This article deals with the topic of damping the rates of a satellite after separation from the launcher by sensing the rates with magnetometers or gyroscopes and actually damping it with torquerods or thrusters. In literature problems of this kind are treated by linearization which is not adequate here due to the high nonlinearity of the problem caused by the high gyroscopic torque.
This paper addresses the observability and controllability of the rate dynamics for symmetric satellite bodies. Furthermore, robust stability of any bodies is investigated by means of the Krasovskii–LaSalle principle which is a variant of Ljapunov's Second Method. It is found that – apart from one exception - the system is robustly stable for certain conditions depending only on the gain matrix and not depending on the orbit, moments of inertia or initial conditions. The exception is that of the intuitive case of an equator type orbit, in which the satellite rotates around the magnetic field lines, in this case the satellite's rate cannot be damped.
Several design configurations are analysed with respect to their performance and cost: Rate damping with magnetometers or gyroscopes as sensors, and torquerods and thrusters as actuators. The results are evaluated with respect to the time to reach the desired rate, the propellant and the power equivalent battery mass used. The goal is to use the results to allow an AOCS equipment and architecture trade-off at an early project phase.
The design of the rate damping control of the SWARM project is presented as an example and demonstrated with simulations.

INTRODUCTION

Most satellite missions begin with the same challenges when the separation from the launcher has taken place: Their fast rotation rate must be damped with the limited power of the battery, before it can be recharged with the solar arrays.
During this phase the rotational rate is measured in many cases with gyroscopes which allow to measure the rate in all three body axes. The rate signal is transmitted to the controller which commands the actuators to create a break torque, again in all three body axes. However, outside of the USA, ITAR restrictions and costs related to gyroscopes may be prohibitive for the mission and forces the designer to look for alternative solutions.
One alternative to gyroscopes for the problem considered in this paper are *magnetometers*. This design choice was made for instance by the SWARM mission [2]. Magnetometers are less complicated equipments and significantly cheaper than gyroscopes and are offered by many suppliers worldwide. However, magnetometers can only simultaneously measure the rate in the *two* axes perpendicular to the Earth magnetic

[1] ESA, ESTEC – Keplerlaan 1, 2201 AZ Noordwijk, The Netherlands - Email: peter.zentgraf@esa.int
[2] Astrium GmbH, D-88039 Friedrichshafen, Germany - Email: domenico.reggio@astrium.eads.net

field lines. The rate component about the magnetic field line themselves cannot be measured. But luckily, while the satellite travels on its orbit it "sees" the field lines from all different angles and thus throughout the orbit will be able to provide measurements of the rate about all *three* axes.
Similarly, on the actuator side, due to the strength of the magnetic field in Low Earth Orbits (LEO) *torquerods* are an alternative actuator to thrusters and wheels for the rate damping after separation. But these suffer in an analogous manner to the magnetometers from the direction of the magnetic field.
Intuitively, rate damping using magnetometers will take longer than rate damping using gyroscopes. But how much longer will it take? And even more fundamental: Is the *heuristic* reasoning for using magnetometer derived rate signals also *mathematically* correct? In other words, are there for instance any initial conditions which in combination with the orbit plane may lead to loss of controllability, observability or even instability?
There are many references on the control of satellites using magnetometers and/or torquerods, for instance [1]. However, in these the plant models are linearised, which is suitable for many cases, but which does not appear to be appropriate for the investigation of initial rate damping, since at separation the rates and the non-linear gyroscopic torque are very large and any linearization would generate in general – i.e. for an arbitrary moments of inertia matrix (MOI) - large modeling errors.
The paper is organized as follows:

- The observability and controllability is investigated for a certain type of MOI matrix of satellites, which can be described as a linear time-varying system.
- A control strategy for rate damping and Sun acquisition is proposed, and stability is investigated for satellites with any MOI matrix.
- With this strategy several sensor and actuator configurations (gyroscopes or magnetometers together with thrusters and torquerods of different size) are analysed with respect to (wrt) the time which is needed to accomplish rate damping and the mass penalty (H/W, fuel, battery mass) which is needed to achieve that performance.

PROBLEM STATEMENT

The system equation of a rigid body is described by the well-known Euler equation

$$\begin{aligned} I\dot{\omega} + \omega \times I\omega &= \tau \\ y &= C(t)\omega + \eta \end{aligned} \tag{1}$$

in which

- I is the 3x3 moment of inertia matrix,
- ω is the 3x1 rate vector of the satellite,
- τ is the 3x1 vector of sum of control torque and disturbances,
- y is the 3x1 measurement signal vector
- $C(t)$ is the 3x3 time varying measurement matrix and
- η is the 3x1 perturbation term vector

For the system described in Eq. (1) the task is to damp the rate ω for a given initial condition ω_0. It is assumed as it was the case for SWARM, that for these high rates the nominal attitude sensor measurements during the separation phase cannot be used,

otherwise the rates could be completely derived. After the rate is small enough the satellite rotates to acquire an attitude such that its solar arrays provide sufficient power. The time needed for that is much smaller than the time to damp the rate. Therefore, and also because it depends on the acquisition strategy itself, this phase is neglected here.
In the first instance the rotational rate of the satellite shall be measured with magnetometers only. Magnetometers measure the Earth magnetic field *b* wrt the body frame of the satellite. In general, the change of a vector wrt time expressed in one frame can be expressed in another frame rotating wrt the first one by [1]

$$\underbrace{\left.\frac{d\bar{b}}{dt}\right|_{inertial}}_{\bar{b}'} = \underbrace{\left.\frac{d\bar{b}}{dt}\right|_{body}}_{\dot{\bar{b}}} + \omega \times \bar{b} \tag{2}$$

in which $\bar{b} = \frac{b}{|b|}$ is the Earth magnetic field *unit* vector and ω is the rate with which the body frame rotates wrt the inertial frame. Multiplying Eq. (2) with the cross product matrix of $\bar{b}$, $\tilde{\bar{b}}$[3], yields

$$-\tilde{\bar{b}}\dot{\bar{b}} = -\left(\tilde{\bar{b}}\right)^2 \omega - \tilde{\bar{b}}\bar{b}' \tag{3}$$

The signal $\tilde{\bar{b}}\dot{\bar{b}}$ is the measured rate signal ω_{meas}: The signal $\bar{b}$ is measured by the magnetometers and its derivative wrt the body frame, $\dot{\bar{b}}$, is derived on-board by numerical differentiation; reformulating Eq. (3) yields

$$\omega_{meas} := -\tilde{\bar{b}}\dot{\bar{b}} = \underbrace{\left[E - \bar{b}(t)\bar{b}^T(t)\right]}_{C(t)}\omega - \tilde{\bar{b}}\bar{b}' \tag{4}$$

in which *C(t)* is the time varying *measurement matrix*. As it can be seen from Eq. (4), the rate measurement signal ω_{meas} is composed of two parts:

1. The <u>ideal signal</u> $\left[E - \bar{b}(t)\bar{b}^T(t)\right]\omega$ which yields the true body rate without the component around the magnetic field $\bar{b}$,
2. And a <u>perturbation signal</u> $-\tilde{\bar{b}}\bar{b}'$ describing the *inertial* change of the magnetic field. This signal is bounded in magnitude and its value depends only on the orbit and neither the attitude nor the rate. It can be considered as a bounded perturbation contributor to the ideal rate signal.
   For instance, in SWARM with an orbit inclination of 88 deg and >300 km altitude this value is about 0.2 deg/s, thus defining the maximum accuracy of the rate determination using magnetometers alone. For an equator orbit with idealized dipole Earth magnetic field model – where the magnetic field vector would inertially constantly point parallel to the Earth rotation axis – the value is zero,

[3] The cross product matrix $\tilde{a}$ is a notation defined such that the matrix-vector product $\tilde{a}v$ yields the same result as with the cross vector product $a \times v$, where *v* is an arbitrary vector.

see Figure 1. However, then the rate can never be determined around this inertial constant axis, similar to rate control using Sun sensors.

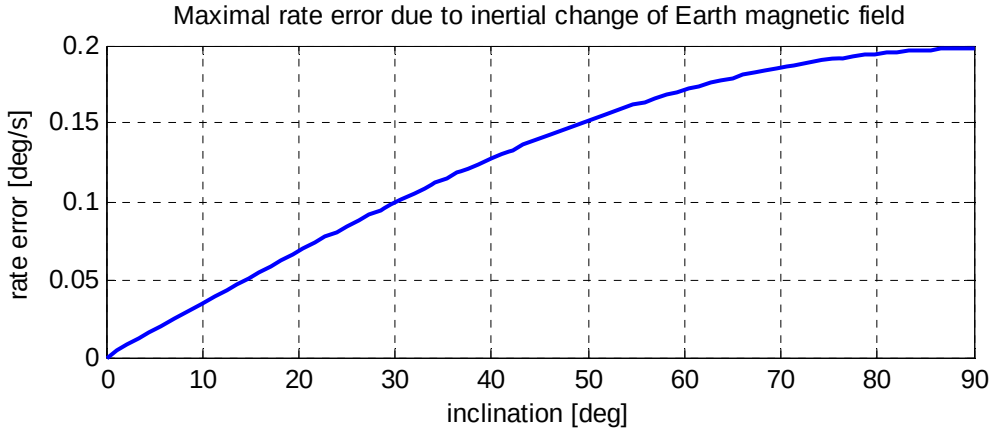

Figure 1. Maximal Rate Measurement Error in one Orbit due to Change of Idealized Earth Magnetic Dipole Model Versus Orbit Inclination Angles.

As far as the actuators are concerned, torquerods generate only control torques τ perpendicular to the Earth magnetic field, whereas thrusters or wheels generate torques around all three body axes.

To summarize, the non-linear system equations in Eq. (1) can be written for different sensor/actuator configurations as follows:

$$\begin{aligned} I\dot{\omega} &= -\tilde{\omega} I\,\omega + B\tau \\ \omega_m &= C\,\omega + \eta \end{aligned} \tag{5}$$

where η is the bounded rate measurement noise. The type of input control matrix, *B,* and the type of measurement matrix, *C,* depend on the sensor/actuator configuration according to table Table 1, in which *E* represents the *3x3* unity matrix.

Table 1. Values for (B,C) Matrices Depending on Sensor/Actuator Configuration.

		B-matrix of Actuators	
C-Matrix of Rate Sensors		***Thrusters or wheels***	***Torquerods***
	Gyroscopes	$B = E; C = E$	$B = E - \bar{b}(t)\bar{b}^T(t); C = E$
	Magnetometer	$B = E; C = E - \bar{b}(t)\bar{b}^T(t)$	$B = E - \bar{b}(t)\bar{b}^T(t); C = E - \bar{b}(t)\bar{b}^T(t)$

OBSERVABILITY AND CONTROLLABILITY

In order to more readily analyze the observability of the system using magnetometers and torquerods the shape moments of inertia matrix is restricted to "cigar-type" symmetric body around the x-axis, i.e. two entries of the matrix are the same:

$$I = \begin{bmatrix} I_x & 0 & 0 \\ 0 & I_p & 0 \\ 0 & 0 & I_p \end{bmatrix} \text{ and } I_x \le I_p \tag{6}$$

Note that the SWARM MOI matrix has a very similar form, which is also typical for a large class of LEO satellites:

$$I_{SWARM} = \begin{bmatrix} 60 & 5 & 20 \\ 5 & 1200 & 5 \\ 20 & 5 & 1220 \end{bmatrix} kg\,m^2 \tag{7}$$

Then the system can be written without modelling errors wrt Eq. (1) as linear time-varying system [4]

$$\begin{aligned} \dot{\omega} &= A\,\omega + B(t)\,u \\ \omega_m &= C(t)\,\omega + \eta \end{aligned} \tag{8}$$

where

$$A = \underbrace{\frac{I_p - I_x}{I_p}\,\omega_{x0}}_{=:\,\omega_p} \begin{bmatrix} 0 & 0 & 0 \\ 0 & 0 & -1 \\ 0 & 1 & 0 \end{bmatrix} = \text{constant and } \omega_{x0} = \omega_x(t=0) \tag{9}$$

and

$$u = \begin{bmatrix} 1/I_x & 0 & 0 \\ 0 & 1/I_p & 0 \\ 0 & 0 & 1/I_p \end{bmatrix} \tau \tag{10}$$

observability for Linear Time-Varying Systems

A condition for observability of time-varying systems can be found in [5]:
Theorem: *A linear time-varying system is "completely" observable in the time interval [t_0, t_1] iff the "observability gramian" M(t_0, t_1),*

$$M(t_0, t_1) = \int_{t_0}^{t_1} \Phi^T(t, t_0) C^T(t) C(t) \Phi(t, t_0)\, dt\,, \tag{11}$$

is non-singular.
The 3x3 matrix $\Phi(t, t_0)$ is the transition matrix.

Note that "completely" observable means that any possible initial state is observable.
It can be shown [5] that if the system is observable in *[t_0, t_1]*, then it is also observable in *[t_0, t_2]* for any $t_2 > t_1$. This is very practical, since the gramian Eq. (10) needs to be evaluated for one t_1 only.

Duality of observability and controllability

Under certain conditions of the system matrices as given below the observability implies controllability and vice versa in [5]:
Theorem: If *a linear time-varying system is observable and if the system matrices hold the following equations true*

$$\begin{aligned} A(t) &= -A(t)^T, \\ B(t) &= C(t)^T, \end{aligned} \tag{12}$$

then the system is also controllable.
Note: As it can be seen from Eq. (9) and Table 1, this is the case here. If the rate is observable then it is also controllable via magnetic torquerods.

Computation of observability Gramian

In order to compute the observability Gramian the transition matrix $\Phi(t,t_0)$ (using Eq. (9)) and the measurement matrix *C(t)* need to be computed:

$$\Phi(t,t_0) = e^{A(t-t_0)} = \begin{bmatrix} 1 & 0 & 0 \\ 0 & \cos\omega_p(t-t_0) & -\sin\omega_p(t-t_0) \\ 0 & \sin\omega_p(t-t_0) & \cos\omega_p(t-t_0) \end{bmatrix} \tag{13}$$

$$C(t) = \left[E - \frac{T_i^b(t) b^i(t) b^{iT}(t) \left(T_i^b(t)\right)^T}{b^{iT}(t) b^i(t)} \right] \tag{14}$$

where a simple dipole Earth magnetic field model is assumed [1], i.e.

$$b^i = \frac{k}{R^3}\left[E - 3r^i\left(r^i\right)^T\right]m^i \tag{15}$$

with

- m^i as idealized dipole vector [0 0 1], k is a constant and
- r^i the position unit vector in a circular orbit with radius R expressed in inertial frame – because of the symmetry to the magnetic field all orbits are distinguished by the inclination angle i .

It is shown in [6] that the transformation matrix T_i^b in Eq. (14) from inertial frame to body frame can analytically be computed for any initial attitude and rate and any moments of inertia matrix as defined in Eq. (6) by

$$T_i^b = Rotate(\omega_p t, e_x) * Rotate\left(\frac{|I\omega_0|t}{I_p}, \frac{I\omega_0}{|I\omega_0|}\right)\left(T_i^b\right)_0 \tag{16}$$

in which

- *Rotate(angle, axis)* defines the rotation of one frame about a given *axis* and an *angle,*
- ω_0 is the initial rate,

- $\left(T_i^b\right)_0$ is the initial attitude of the body frame wrt the inertial frame.

Inserting Eqs. (13)-(16) into Eq. (11) allows to compute the Gramian M with 8 scalar independent variables ω_0, $\left(T_i^b\right)_0$, moments of inertia ratio I_x/I_p, and inclination angle i. Unfortunately the singularity of M can only be analyzed numerically. As a measure of matrix singularity the minimal singular value $\sigma_{\min}(M)$ is used:

$$\chi := \underbrace{\min}_{\omega_0, \left(T_i^b\right)_0, \frac{I_x}{I_p}, i} \left\{\sigma_{\min}(M)\right\} \tag{17}$$

If χ is zero, M is singular, otherwise M is not singular.

The approach is checked with a simple *test*: A satellite flying an equator orbit (*i=0 deg*), with initial attitude $\left(T_i^b\right)_0 = E$, with initial rate around the inertial z-axis (for instance ω_0*=[0 0 5] deg/s*) cannot be observable, because it rotates around the magnetic field throughout the orbit from $t_0=0$ and $t_1=2\pi/T_{orb}$ (T_{orb} is the time to travel one full orbit). This should be reflected in the evaluation of χ in Eq. (17). Computing χ yields $\chi = 0$, which was expected. Thus, M is singular and the system defined in Eq. (8) is not observable and the approach passed the test.

For a practical example χ is computed in the following three steps:

1. Define meaningful lower and upper bounds for the free variables to cover the SWARM mission [2]:
   a. 0.3 deg/s < $|\omega_0|$ < *10 deg/s*
   b. 0.5 * $(I_x/I_p)_{nominal} < I_x/I_p <$ 12* $(I_x/I_p)_{nominal}$ ($(I_x/I_p)_{nominal}$ = *30/1200* from Eq. (7)
   c. *80 deg< i < 90 deg*
   d. All possible directions for ω_0 and for the initial attitude $\left(T_i^b\right)_0$ are considered.
2. Perform a parameter study with 10^6 combinations of the free variables given in a.-d. and find smallest χ
3. For a practical approach, use this value as starting point for non-linear constrained optimization (Matlab function *fmincon* [7]) to find a local minimum. We are aware that possible other algorithms may find the global minimum.

For the SWARM case this yields a result of $\underline{\chi=0.9899}$ for the variable given in Table 2:

Table 2. Results of minimization to determine χ.

Variables	***Values***
ω_{0_min}	[0.0739 -0.1381 0.2559] deg /s
$\left(T_i^b\right)_{0\_min}$	0.6866 -0.1827 0.7037 -0.1998 0.8832 0.4243 -0.6990 -0.4319 0.5699
I_x/I_{p_min}	0.5 * $(I_x/I_p)_{nominal}$
$i_{\_min}$	80.0021 deg

As an example in Figure 2 is the 3-dimensional plot of χ around its minimum on two of the eight variables shown. The "carpet"-type shape of the figure indicates that the influence of the moments of inertia ration has much less influence on the gramin than the rate.

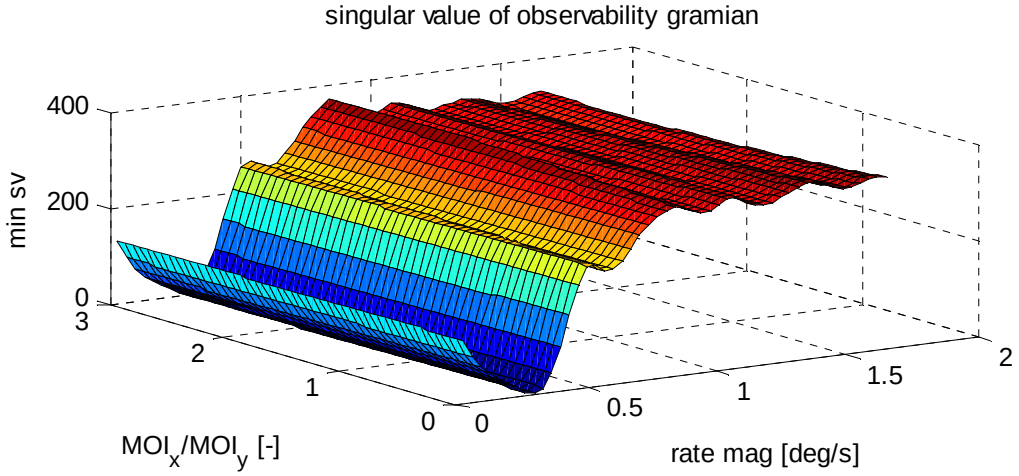

Figure 2. Singularity measure χ of *M* around its minimal value for varying I_x/I_{p_min} and $|\omega_0|_{\_min}$

Conclusions on observability and controllability

M is non-singular (since χ>0.9899) wrt the considered variable range (any initial attitude, any rate direction and any rate magnitude between *0.3* and *10 deg/s* and inclination angles between *80* and *90 deg*) and thus, the system defined in Eq. (8) is observable as well as controllable.

STABILITY OF RATE DAMPING CONTROL

The stability of the system Eq. (5) is investigated by means of the Krasovskii–LaSalle principle [8]:

Krasovskii–LaSalle principle [8]:
Given a representation of the system, $\dot{x}(t) = f(x)$, *where x is the vector of variables, with* $f(x=0) = 0$.
If a continuous differentiable (Lyapunov) function $V(x)$ *can be found such that*

- $V(x) > 0$ *(positive definite)*
- $\dot{V}(x) \le 0$ *(negative semi definite)*

and $V(x=0) = \dot{V}(x=0) = 0$
and if the set $\{\dot{V}(x=0)\}$ *contains no trajectory of the system except the trivial trajectory* $x(t) = 0$ *for* $t \ge 0$, *then the origin* $x(t) = 0$ *is globally asymptotically stable.*

The Krasovskii–LaSalle principle is in fact a relaxation of Ljapunov's Second Method [9], because it allows $\dot{V} \le 0$ whereas Ljapunov's Second Method strictly requires $\dot{V} < 0$.

The basic idea of the stability investigation is to determine the set of all trajectories x_1 for which $\dot{V}(x_1) = 0$ and to check if x_1 is a possible trajectory of the system, i.e. is $\dot{x}_1(t) = f(x_1)$ a true equation or not.

Construction of Lyapunov's Function

The Lyapunov function is selected to be

$$V = \frac{1}{2}\omega^T I\omega > 0 \text{ for } |\omega| > 0 \tag{18}$$

which is only zero for $|\omega|=0$.
The derivative is expressed by inserting the system equations Eq. (8)

$$\begin{aligned} \dot{V} = \omega^T \quad & \underbrace{I\dot{\omega}} \quad = \underbrace{\omega^T \tilde{\omega} I\omega} + \omega^T B\tau = \omega^T B\tau \\ & = -\tilde{\omega} I\omega + B\tau \qquad = 0 \end{aligned} \tag{19}$$

The control law used for damping the rate is a simple proportional controller using Eq. (8):

$$\tau = -K_d \omega_m = -K_d C\omega \tag{20}$$

The derivative of the Lyapunov function can now be written as

$$\dot{V} = -\omega^T B K_d C\omega \tag{21}$$

Using magnetometers and torquers as the most "challenging" configuration gives with the corresponding *B* and *C* matrices from Table 1:

$$\dot{V} = -\omega^T \underbrace{\left(E - \bar{b}\bar{b}^T\right) K_d \left(E - \bar{b}\bar{b}^T\right)}_{=: P} \omega \tag{22}$$

Note that $\dot{V}$ does not depend on the moments of inertia matrix *I*, and thus not on any changes or uncertainties of *I*.
Now the question is under which circumstances, i.e. for which trajectory *ω(t)*, the matrix *P* can become positive semi-definite, because then $\dot{V} \le 0$. Consider the following properties:

- The matrix $\left(E - \bar{b}\bar{b}^T\right)$ has for any magnetic field unit vector $\bar{b}$ rank 2. It can easily be seen that the eigenvector corresponding to the eigenvalue zero is $\bar{b}$.
- If the choice of K_d is restricted to symmetric, positive definite matrices, then it can be decomposed into the product of a full rank matrix *S* and its transpose, $K_d = SS^T$, and the matrix *P* in Eq. (22) can be similarly decomposed into

$$P = \left[S\left(E - \bar{b}\bar{b}^T\right)\right]^T \left[S\left(E - \bar{b}\bar{b}^T\right)\right] \tag{23}$$

  This means that *P* has the same rank as matrix $\left[S\left(E - \bar{b}\bar{b}^T\right)\right]$ which has rank *2*, and therefore matrix *P* has exactly one eigenvalue zero and the corresponding eigenvector is $\bar{b}$.

This means that it needs to be checked if it is possible to have a trajectory of the kind

$$\omega_1(t) = c(t)\,b(t) \tag{24}$$

with a free selectable time-varying scalar function *c(t)*, because then

$$\dot{V} = -c\,b^T\left(E - \bar{b}\bar{b}^T\right)K_d\left(E - \bar{b}\bar{b}^T\right)c\,b = -c\,b^T\left(E - \bar{b}\bar{b}^T\right)K_d\,c\left(b - b\right) = 0 \tag{25}$$

and the system is not globally asymptotically stable. This is also the *only* possible candidate which can cause $\dot{V} = 0$.

To investigate if the candidate trajectory in Eq. (24) is a possible system trajectory it is differentiated and inserted into Eq. (5) to give:

$$\begin{aligned} I\dot{\omega}_1 &= -\tilde{\omega}_1 I\omega_1 \\ \Leftrightarrow \quad I\,\dot{c}b + I\,c\dot{b} &= -c^2\tilde{b}\,I\,b \end{aligned} \tag{26}$$

The candidate trajectory ω_1 in Eq. (24) is then a possible trajectory if a scalar function *c* can be derived which solves the vector equation Eq. (26).

Two main cases are distinguished now, namely that *b* is an eigenvector of *I* and that *b* is <u>not</u> an eigenvector of *I*:

1. Case $I\,b \neq \lambda b$

   In this case is $\tilde{b}\,I\,b \neq 0$. If a scalar function *c* solves Eq. (26), then it will also solve for the b^T and $b^T I$ projections – in other words left-multiplications - of Eq. (26). If for these projections no scalar function *c* can be derived, then there will be also no solution for Eq. (26):

$$\begin{aligned} b^T * \text{Eq.}(26): &\quad \dot{c}b^T Ib + cb^T I\dot{b} = 0 \rightarrow \dot{c}/c = -b^T I\dot{b}/b^T Ib \\ b^T I * \text{Eq.}(26): &\quad \dot{c}b^T I^2 b + cb^T I^2\dot{b} = 0 \rightarrow \dot{c}/c = -b^T I^2\dot{b}/b^T I^2 b \end{aligned} \tag{27}$$

   Rearranging Eq. (27) yields

$$b^T I\dot{b}/b^T Ib = b^T I^2\dot{b}/b^T I^2 b \Leftrightarrow b^T I\dot{b}/b^T I^2\dot{b} =: 1/\alpha = b^T Ib/b^T I^2 b \tag{28}$$

   where the arbitrary scalar α has been introduced. Eq. (28) can be written in two equations

$$\dot{b}^T I\left(I - \alpha E\right)b = 0 \tag{29}$$

$$b^T I\underbrace{\left(I - \alpha E\right)}_{=:J}b = 0 \tag{30}$$

   Eq. (30) can only be true if the matrix product *I*J* has an eigenvalue zero and *b* is the corresponding eigenvector. Since *I* is positive definite, *I*J* can only have a zero eigenvalue if *J* has a zero eigenvalue. *J* only has a zero eigenvalue if α is an eigenvalue of *I,* and only if *b* were then the corresponding eigenvector to α the product *I*J*b* is zero. But this would mean that *b* is required to be the eigenvector of *I* – a case which has been explicitly *excluded* here!

   To conclude, Eq. (30) cannot be solved, and thus neither Eq. (26), and thus is ω_1 in Eq. (24) not a system trajectory that solves Eq. (5).

2. Case $I\,b = \lambda b$

In this case is $\tilde{b} I b = 0$. Then Eq. (26) can be rewritten as

$$\begin{aligned} & I\left(\dot{c}b + c\dot{b}\right) &= 0 \\ \Leftrightarrow \quad & \dot{c}b + c\dot{b} &= 0 \end{aligned} \tag{31}$$

From kinematics of derivatives in rotating systems

$$\dot{b} = \underbrace{-\tilde{\omega}_1 b}_{0} + b' = b' \tag{32}$$

where b' is the derivative in the inertial frame, Eq. (31) can be written as

$$b' = -\frac{\dot{c}}{c} b \tag{33}$$

Solving Eq. (33) for *b* yields

$$b(t) = b_0 \underbrace{\exp\left(\int_{t_0}^{t} -\frac{\dot{c}(s)}{c(s)} ds \right)}_{scalar > 0} \tag{34}$$

In other words, in an orbit where the Earth magnetic field <u>does not change its direction</u> the candidate trajectory ω_1 in Eq. (24) is in deed a possible trajectory. The only orbit where the magnetic field evolves over time as shown in Eq. (34) is a near equator orbit, where the field lines are throughout the mission life time parallel to the inertial z-axis. Then and only then, the trajectory

$$\omega_1(t) = c\, b_0 \tag{35}$$

will not decrease the Lyapunov function *V* and the rate will not be reduced. This case is already evident from intuition. The news is that this is the *only* constellation where this can happen.

Only in a near equator orbit the system defined in Eq. (5) and (20) might not be globally asymptotically stable. This is then the same situation as if the rate should be measured with sun sensor measurements only. However, in practice LEO missions do not fly in such an orbit.

Impact of Remaining Equipment Configurations on Stability

So far stability has been shown when magnetometers are used as sensors and torquerods are used as actuators. From Table 1 remain three configurations to be checked:

1. <u>Gyroscopes & Thrusters</u>
   The *P*-matrix in Eq. (22) is reduced to the controller gain matrix K_d. If this matrix is selected positive definite, global asymptotical stability is of course ensured even for the near-equator orbit.
2. <u>Gyroscopes & Torquerods</u>
   The *P*-matrix in Eq. (22) becomes now unsymmetrical:

$$\dot{V} = -\omega^T \underbrace{\left(E - \bar{b}\bar{b}^T\right)K_d}_{=: P_2}\omega \tag{36}$$

For this case the new candidate trajectory for which the Lyapunov function might not shrink is

$$\omega_2(t) = c(t)\underbrace{\left(K_d\right)^{-1} b(t)}_{=: b_2(t)} \tag{37}$$

Since the controller gain matrix K_d was required to be positive definite its inverse always exists.

The previously performed analysis on the magnetometer/torquerod configuration did not make any assumption on a magnetic field vector *b*. Therefore, the analysis is also valid for a magnetic field vector $b_2 = \left(K_d\right)^{-1} b$, which is only a scaling of vector *b.* Therefore global asymptotical stability is of course ensured except for a near-equator orbit.

3. Magnetometers & Thrusters

The *P*-matrix in Eq. (22) becomes again unsymmetrical:

$$\dot{V} = -\omega^T \underbrace{K_d\left(E - \bar{b}\bar{b}^T\right)}_{=: P_3}\omega \tag{38}$$

The only trajectory that may cause $\dot{V} = 0$ is the same as in Eq. (24),

$$\omega_1(t) = c(t)\, b(t) \tag{39}$$

therefore the same analysis and the same conclusion hold.

Impact of Limiters on the Approach

For stability to be ensured the only requirement on the controller gain matrix K_d is that it is positive definite – it does not mean it cannot be time varying, but it must remain positive definite.

Therefore, *vector limiters* which limit the magnitude of the desired torque but remain its direction are of no stability concern: A new, fictitious controller gain matrix K_{d2} can be expressed by the old matrix K_d divided by the factor, for which the desired torque exceeds the vector limiter. This multiplication does not change the positive-definite property of the controller gain matrix K_d and thus not the stability.

The second type of limiters, *axis limiters*, do not maintain the torque direction but limit the maximal values in each axis. The argument here is similar. Say $\tau_{c\,sat}$ is the saturated torque in any axis, and $\tau_{c\,des}$ (no zero entries assumed in this example) was the desired torque we wanted to have originally. Then for instance one possible positive definite gain matrix which will map one torque into the other is K_d^* as given below:

$$\tau_{c\,sat} = \underbrace{diagonal\left\{\frac{\tau_{c\,sat\,x}}{\tau_{c\,des\,x}}, \frac{\tau_{c\,sat\,y}}{\tau_{c\,des\,y}}, \frac{\tau_{c\,sat\,z}}{\tau_{c\,des\,z}}\right\}}_{K_d^*} \tau_{c\,des} \tag{40}$$

Conclusions on Stability

Note that no assumption was made on a specific model of the magnetic field. Global asymptotical stability is achieved when the rates are measured using magnetometers and/or the torques are commanded using torquerods. Only in one case this property might get lost: When the satellite flies in an orbit where the direction of the magnetic field does not change inertially, stability cannot be shown. This may in theory only happen in a near equator orbit, but in practice this is unlikely, since the real geomagnetic field is not perfect symmetric.

WORST CASE RATE DAMPING IN AN IDEALIZED ENVIRONMENT

This section compares the rate damping performances with different sensor / actuator configurations, as well as different sensor signal types and thruster and torquerod sizes. SWARM mission parameters are assumed here using a simple, idealized model.

Measures for Performance and Cost

The performance measure is the *time* needed to damp out a rate magnitude of 8.67 deg/s (5 deg/s in all axes) down to a magnitude of 0.5 deg/s.
The cost measure in order to reach the performance is the *mass.* Two types of masses are distinguished:

1. The "static" mass which comprises all mass needed to use either thrusters (i.e. the mass needed for tanks, feed module, thruster pipe work, tank support, thruster support and of course the fuel needed for initial rate damping) or the mass of three torquerods. If thrusters are mandatory for orbit control, then here the total allocated fuel for attitude control should be counted.
2. The "dynamic" mass which means the battery mass which is needed to provide the energy, i.e. the power during rate damping; as conversion factor the one for Lithium batteries (300 W hr/kg) is taken as realistic value [12]. Since it is possible that the battery size is driven by large payload needs the dynamic mass computed for rate damping might be already included in the battery sizing, and is listed separately.

Equipment configurations

In total 4 different sensor signals and 5 different actuators are used, i.e. 20 combinations are checked and compared. To be more realistic, key parameters from existing equipments are used.
The characteristics of the usage of the different units are explained as follows:

1. Sensors

In total, 4 different sensor signals are generated from 2 units:

a. *Magnetometer*: As a possible unit the properties from the LusoSpace unit [13] are used to derive the cost.
   The impact of three different rate signals is investigated:

i. The measurement of the magnetic field is differentiated with a simple discrete differentiator, and the cross product with the measurement, $\dot{\bar{b}} \times \bar{b}$, is used as rate measurement signal.
ii. In order to check the impact of the accuracy of the differentiation, the best possible signal that a filter on board could derived is used, namely the right hand side from the kinematic equation of Eq. (4), $\omega_m = \left(E - \bar{b}\bar{b}^T\right)\omega + \bar{b}' \times \bar{b}$. This signal is derived from the physical simulator and fed directly into the onboard-part of the simulator.
iii. The ideal 2-axis measurement rate measurement without the component around the magnetic field vector is taken as a reference only. Clearly, this signal could never be derived onboard.

b. *Gyroscope*: The cost properties from the MEMS gyroscope [14] is used to derive the costs.

2. *Actuators*

In total, 5 different actuator configurations using 3 different actuator units are compared. The maximal possible torque is computed by a constrained optimization routine [7].

a. The 100 Am^2 torquerods from Dutch Space are used to represent a medium size[15].
b. In order to represent a large size, the properties of the 100 Am^2 torquerods are used for a fictitious unit of 150 Am^2.
c. As an extreme large torquerod the 700 Am^2 unit from Dutch Space is used.
d. For medium sized thrusters, the one from Bradford [16] are used as they are accommodated for SWARM.
e. In order to represent a large sized thruster, the same properties of the medium sized thrusters are used but their distance wrt the COG position is doubled to get double torque capacity.

The configurations are summarized in Table 3.

Table 3. Sensor/Actuator Configurations Used in the Analysis.

	Unit	***"static" mass***	***Power needs***	***Usage Characteristic***	***Name***
Sensors	Magneto meter LusoSpace [13]	2*0.3 kg	1 W	Measurement signal $\omega_m = \dot{\bar{b}} \times \bar{b}$ derived from discrete differentiator.	MAG simple
				Best possible signal is used, see Eq. (4).	MAG best
				Ideal 2-axis rate signal is used, see Eq. (4).	MAG ideal
	MEMS gyros [14]	2*0.8 kg	4 W	Full 3-axis rate information is used.	GYR

	Unit	*"static" mass*	*Power needs*	*Usage Characteristic*	*Name*
Actuators	Torquerod 100 Am^2 [15]	3*2.7 kg	0.24 A, 50 Ohm	Maximal possible torque **6.5 mN**	MTQ M
	Torquerod 150 Am^2[15]	3*2.7 kg	0.24 A, 50 Ohm	Maximal possible torque **9.7 mN**	MTQ L
	Torquerod 700 Am^2[15]	3*9.1 kg	0.828 A, 54 Ohm	Maximal possible torque **45.3 mN**	MTQ XXL
	Thrusters Bradford [16]	30.36 kg dry mass	Power hold 1W; Power initiate off-on switch 8W for 0.06 s;ISP=43 s	Maximal possible torque **69 mN**	THR M
				Maximal possible torque **138 mN**	THR L

Modeling Assumptions

All simulations are performed in Matlab/Simulink [7]. The plant characteristics are modeled using Eq. (1)-(5) and the P-controller from Eq. (20). For the Earth magnetic field a simple dipole model from [1] with a dipole parallel to the Earth rotating axis is used.
The orbit is modeled as a perfect circle with 90 deg inclination.
For the initial conditions, to have the largest possible angular momentum with an initial rotation magnitude of 8.67 deg/s parallel to the magnetic field lines.

Example: Simulation with Different MOI Parameters

Two simulation runs (Nominal, Nominal+Delta) with exactly the same conditions except for different MOI matrices have been performed:

$$I_{Nominal} = \begin{bmatrix} 60 & 5 & 20 \\ 5 & 1200 & 5 \\ 20 & 5 & 1220 \end{bmatrix} kg\,m^2 \; ; I_{Nominal+Delta} = \begin{bmatrix} 1560 & 55 & -380 \\ 55 & 1700 & 45 \\ -380 & 45 & 9220 \end{bmatrix} kg\,m^2 \qquad (41)$$

The result is shown in Figure 3: Even though the MOI parameter changed drastically, stability remains and the corresponding rate damping time is even shorter than the one for the nominal plant. The reason is that the attitude for the nominal case does no longer align the initial rate to the magnetic field lines, since the MOI changed now from Nominal to Nominal+Delta. This demonstrates on one hand the robustness of the stability and on the other hand the large impact of the initial conditions on the rate damping time.

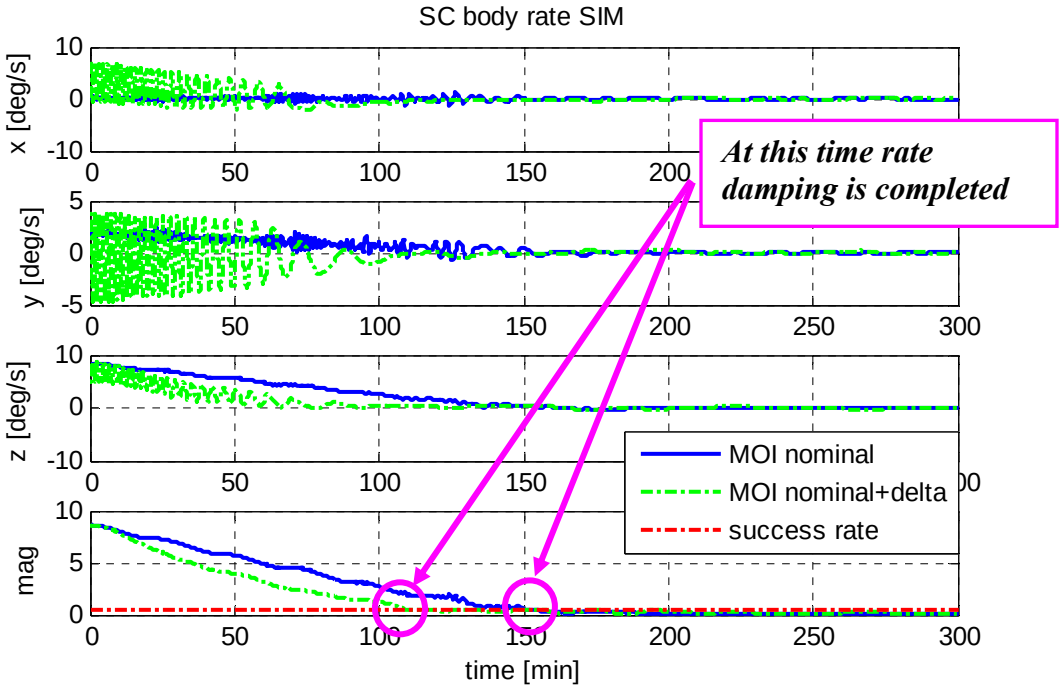

Figure 3. Result of Rate Damping for two different MOI matrices.

Compiled Simulation Results on Rate Damping Performance and Costs

Simulations have been performed for 15 different orbit positions, and the average rate damping time has been recorded for each sensor/actuator configuration. The results are shown in Figure 4. For each torquerod and thruster group two different masses are shown, one without extra battery mass (assuming the battery is large enough anyway) and one with extra battery mass (assuming that the battery would have to be oversized just for the initial rate damping).

The worst damping times are achieved with "MTQ M" and "MTQ L", around 1000 min and 700 min for the different sensor signals, respectively. Since in this case the smallest mass is needed, the Δmass is set to zero. On the other hand, "THR M" and "THR L" give the best result in terms of performance, but they require the largest extra mass penalty– up to **23** kg.

The zoom for "MTQ L" (blue solid line zoom frame) shows that there is no improvement in the performance when the more complex signal "MAG best" is used instead of "MAG simple" – so additional SW effort does not bring any advantage. As expected, the reference signal "MAG ideal" gives a slightly better result. The battery mass could cost an additional 0.5 kg battery mass penalty.

As far as the thrusters "THR M" and "THR L" are concerned (black, dashed zoom frame) the different MAG signals do not show any difference, when gyros are used instead of the MAG signals the rate damping times are halved.

The "MTQ XXL" (orange dashed dotted zoom frame) the different MAG signals show expected order of improvements in rate damping times; gyroscopes generate marginally smaller rate damping times. The extra battery mass could cost 1 kg if not foreseen in the battery mass budget already.

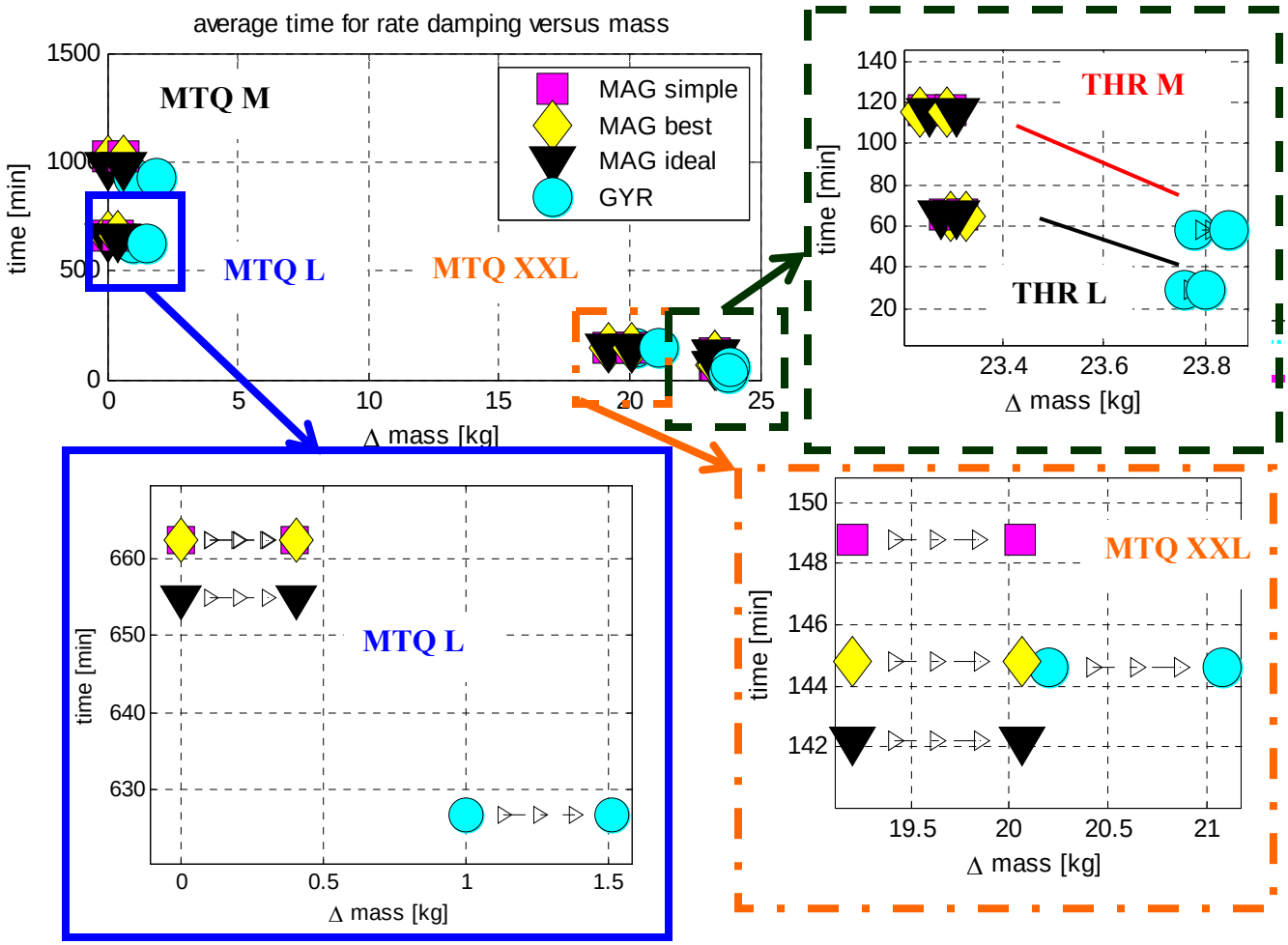

Figure 4. Average Time for Rate Damping versus Delta Mass for Different Configurations.

In Figure 5 the rate damping times are plotted wrt to the maximal torque capability. Clearly, the higher the torque the smaller becomes the damping time. Figure 6 shows that the maximal torque capability is almost inverse proportional to the rate damping time if magnetometers are used, regardless if the actuators are thrusters or torquerods. If thrusters are used, the change from magnetometers to gyroscopes brings a factor of 2 improvement.

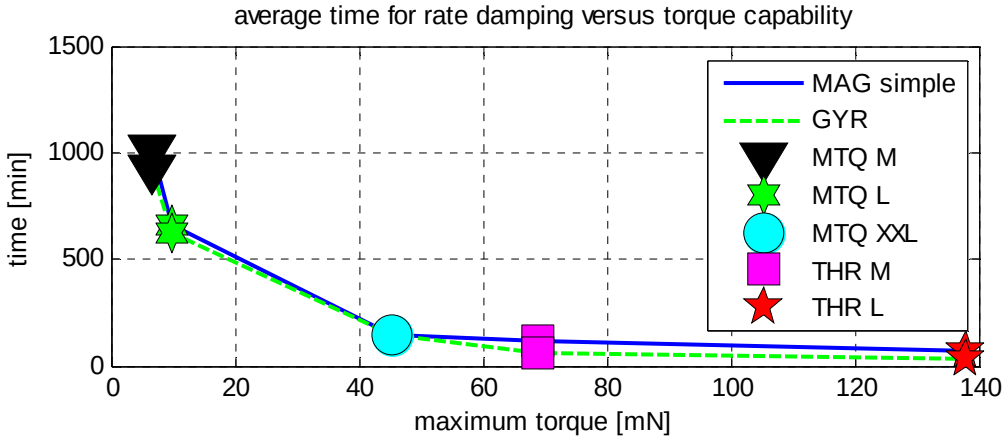

Figure 5. Average Time for Rate Damping versus Torque Capability.

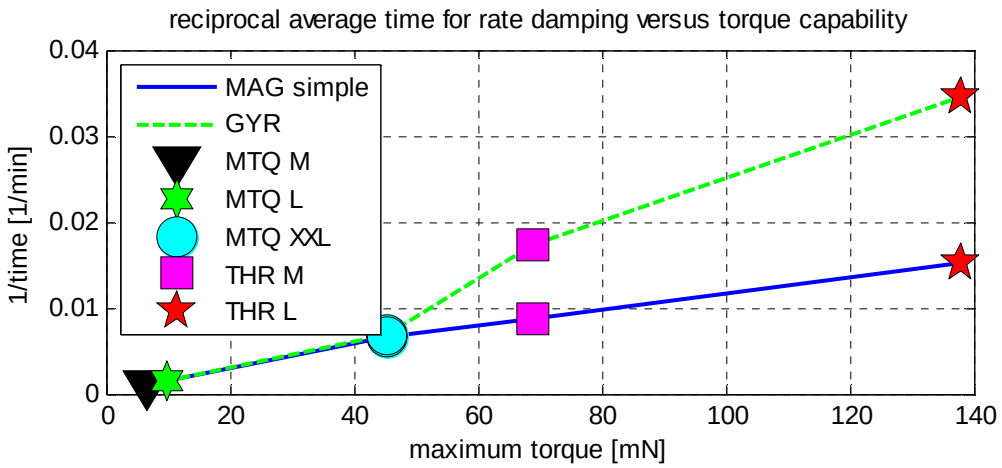

Figure 6. Reciprocal Average Time for Rate Damping versus Torque Capability.

REALIZATION OF RATE DAMPING DESIGN IN AOCS OF THE SWARM MISSION

The SWARM Mission

Swarm provides a survey of the geomagnetic field and its temporal evolution [2].
It consists of 3 identical S/C, 2 satellites flying in parallel between 450 km (BOL) and 300 km (EOL), and 1 satellite at 530 km altitude. With 88° inclination these are near polar orbits.
The nominal attitude has a nadir orientation. Rotation maneuvers of S/C about roll, pitch and yaw are used for instrument calibration and orbit Control. The safe mode is Earth-oriented. Pointing requirements are 2° about all axes, with limitations on use of actuators.

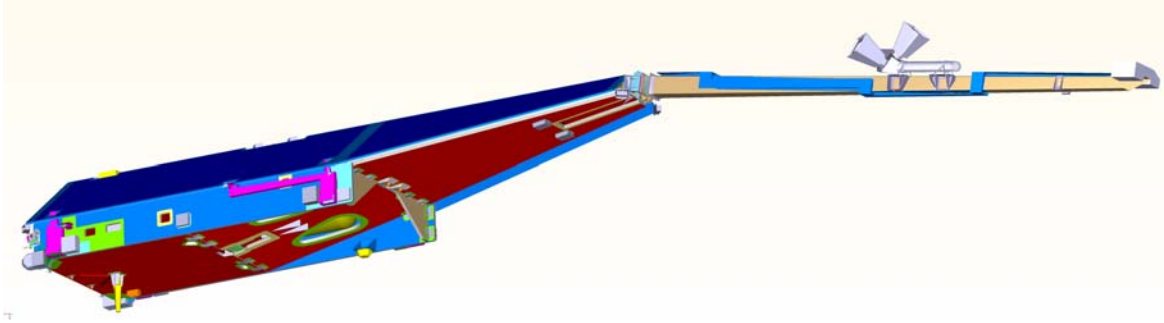

Figure 7. SWARM Satellite

The S/C have a mass of about 500 kg with inertias of 60, 1200, 1220 kgm² about x,y,z. Instruments are mostly mounted on a boom, which after deployment will extend the S/C length to 9.3 m.
The sensors for AOCS are 3 Startracker2 (STR), 1 internal redundant GPS Receiver (GPSR), 1 Coarse Earth & Sun Sensor (CESS) with 6 heads placed orthogonal on the S/C and 3 Magnetometers (FGM) which can be used for rates up to 0.5 deg/s. As actuators 3 Magnetic Torquer (MTQ) each 10 Am² and 24 Cold Gas Thruster (THR), of which 2x8 for attitude control in all 3 axes, each 20 mN force and 2x4 for orbit control, placed in -x and +y direction, each 50 mN force. MTQs and THRs are used by each control mode.
The following control modes are applied:

- Rate Damping: rates are measured by the FGMs, main actuation by THR
- Coarse Pointing: power and thermal safe earth pointing attitude using CESS
- Fine Pointing: STR and GPSR are used for attitude and position knowledge
- Orbit Control: similar to FPM, additionally performing slews for instrument calibration and for orbit change and maintenance which requires using orbit control thruster

Rate Damping Design

The RDM controller is a simple proportional controller on the S/C rate with reference rate zero. The S/C rate is computed by processing and derivation of the FGM measurements.

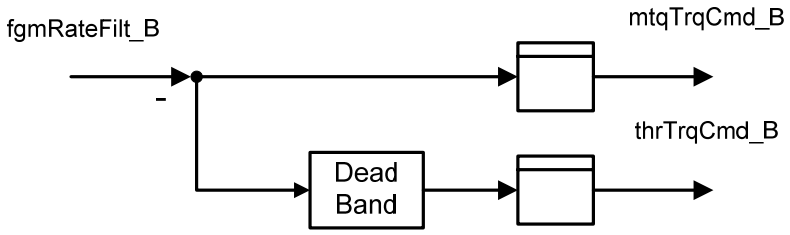

Figure 8. SWARM Rate Damping Controller

The controller outputs the torque commands (corresponding to THR M in Table 3) for the torquerod and the thruster. A dead band for the thruster inhibits the thruster activation for low rates which can be covered by the torquerod.

Worst Case Test Scenarios With Default Configuration

The flaw of this design is the miss of the rate measurement about the magnetic field line. To test this design in worst case, initial conditions are identified where the change of the magnetic field vector is small.

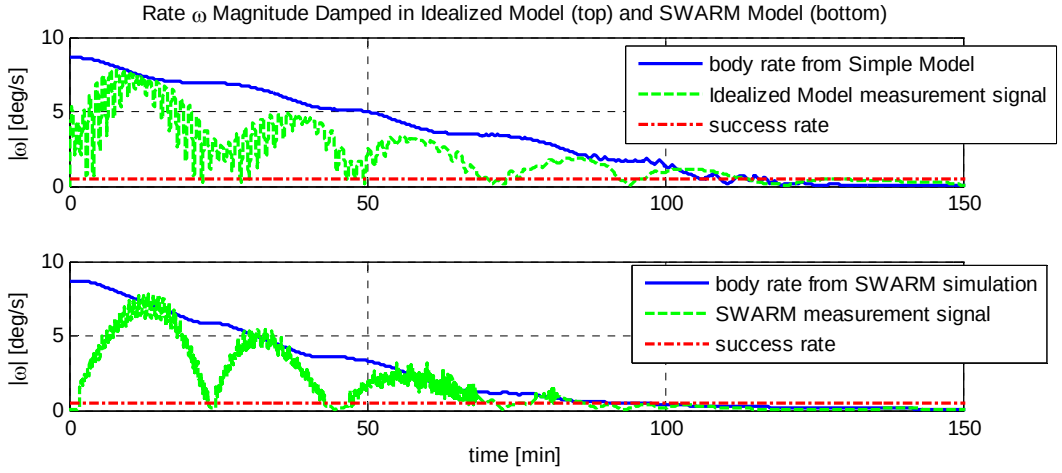

Figure 9. Comparison of Results for Rate Damping with SWARM and with Simple Model

Figure 9 shows on the top plot the result from the simple idealized model used in Figure 3; after 117 min. the rate is damped below 0.5 deg/s The bottom plot of Figure 9 shows the results performed with the complex SWARM model (physics and AOCS) for the

same conditions, in which the rate is damped in 97 min. The results are not identical, since the inhomogeneous part of the magnetic field model) are very different.

CONCLUSIONS

From a control theory point-of-view rate damping with magnetometers using 2-axis measurement is as "safe" as with gyroscopes using 3-axis measurement: Global asymptotical stability is achieved except for the case when the magnetic field does not change. This is only in near-equator orbits possible with perfect field symmetry which is in practice not realistic. The result is confirmed by the evaluation of the observability criterion where no loss of this property could be detected except for the mentioned case. Since SWARM is in a 90 deg inclination orbit, the control concept is "clean".

Irrespective of the actuators used, the simulations show that the rate damping times are almost inverse proportional to the maximum torque capability: Using thrusters, the improvement in rate damping time is a factor of 2 when gyros are used instead of magnetometers.

In general, if rate damping shall be performed fast, then the choice should be a gyroscope/thruster configuration. If rate damping shall be performed cheap, a magnetometer/torquerod configuration can be an alternative, if the magnetic disturbances introduced are acceptable on system level. This result may serve as an input for an overall system evaluation on the mission dependent best possible sensor/actuator configuration.

REFERENCES

[1] T. Pulecchi et al., *Classical vs Modern Magnetic Attitude Control Design: A case Study,* GNC 2008 7th International ESA Conference, Tralee, County Kerry, Ireland, 2008

[2] http://www.esa.int/esaLP/LPswarm.html

[3] J. R. Wertz, *Spacecraft Attitude Determination and Control*, *Kluwer Academic Publishers, 1978*.

[4] P.C. Hughes, *Spacecraft Attitude Dynamics*, *John Wiley & Sons, 1986*.

[5] http://www.eas.asu.edu/~tsakalis/notes/sco.pdf

[6] Lisandro Hernández de la Peña, *Discontinuous molecular dynamics for semiflexible and rigid bodies*, The Journal of Chemical Physics 126, 074105, 2007.

[7] www.mathworks.com

[8] http://en.wikipedia.org/wiki/Krasovskii-LaSalle_principle

[9] http://en.wikipedia.org/wiki/Lyapunov_stability

[10] Gilbert Strang, *Linear Algebra and its Applications*, Harcourt Brace & Company, 1986.

[11] http://en.wikipedia.org/wiki/Positive-definite_matrix#Characterizations

[12] J. R. Wertz and Wiley J. Larson, *Space Mission Analysis and Design*, Third Edition, Space Technology Library, 1999.

[13] www.lusospace.com

[14] http://www.sea.co.uk/docs/MEMS%20DATASHEET%2006.pdf

[15] www.dutchspace.nl

[16] http://www.bradford-space.com